

Article

Impact Analysis of Urban Morphology on Residential District Heat Energy Demand and Microclimate Based on Field Measurement Data

Yanxue Li ^{1,*}, Dawei Wang ¹, Shanshan Li ¹ and Weijun Gao ^{1,2} 

¹ Innovation Institute for Sustainable Maritime Architecture Research and Technology, Qingdao University of Technology, Qingdao 266033, China; wdw0606@foxmail.com (D.W.); lishanshan683@outlook.com (S.L.); weijun@kitakyu-u.ac.jp (W.G.)

² Faculty of Environmental Engineering, The University of Kitakyushu, Kitakyushu 808-0135, Japan

* Correspondence: liyanxue@qut.edu.cn; Tel.: +86-15689978251

Abstract: In this work, we focus on investigating the relationship between urban morphology parameters and residential building space heating energy performance, comparing microclimate conditions of existing residential blocks with central heating supply. Firstly, a dataset composed of district morphological parameters that measured heat energy consumption was established. Then, effects of morphological indicators including cover ratio, average building height, and floor area ratio on building space heating energy efficiency were assessed specifically. Analysis results show that a larger floor area ratio induced a reduction in heating energy consumption density, the observed effect is notable at an initial increase of floor area ratio. Thirdly, the case study shows that the heating load of residential districts with a high built density is more sensitive to solar radiation. To further assess how and to what extent urban forms alter microclimates, on-site measurement investigated detailed changes in the thermal environment of selected residential districts before and after the operational stage of central heating supply. Analysis results demonstrate that heat energy delivered by a central heating supply could dampen the variations of local outdoor air temperatures, more notable for residential districts with a higher floor area ratio during the night period. Findings from this work would be useful for urban planners considering energy-efficient design practices.

Keywords: urban morphology; district heating demand; microclimate; on-site measurement



Citation: Li, Y.; Wang, D.; Li, S.; Gao, W. Impact Analysis of Urban Morphology on Residential District Heat Energy Demand and Microclimate Based on Field Measurement Data. *Sustainability* **2021**, *13*, 2070. <https://doi.org/10.3390/su13042070>

Academic Editor: Baojie He

Received: 20 January 2021

Accepted: 9 February 2021

Published: 15 February 2021

Publisher's Note: MDPI stays neutral with regard to jurisdictional claims in published maps and institutional affiliations.



Copyright: © 2021 by the authors. Licensee MDPI, Basel, Switzerland. This article is an open access article distributed under the terms and conditions of the Creative Commons Attribution (CC BY) license (<https://creativecommons.org/licenses/by/4.0/>).

1. Introduction

The mitigation of greenhouse gas emissions is a key issue in reversing the trend of global climate change, with growing energy consumption and energy-related CO₂ emissions being the main contributors to the challenge. The building sector is responsible for a large proportion of global energy consumption, so improving building energy efficiency is increasingly viewed as having an important role in sustainable development [1,2]. For instance, driven by rapid urbanization over recent decades, the amount of energy used for building space heating in North China shows a sustained annual rising share of final energy consumption—it was responsible for approximately 21% of total building energy consumption in 2018 [3]. As illustrated in Figure 1, in comparison with the developed world, the residential sector of developing countries is in an important position to tackle rising energy consumption due to rapid urban expansion. Therefore, it is important to pay attention to urban community or district design practices from an energy-efficiency and long-term sustainability perspective.

Different energy-saving measures have been implemented in the building sector in a bid to mitigate energy consumption, which can be mainly classified into passive and active energy-saving measures. A number of previous publications draw attention to retrofitting strategies and the exploitation of on-site renewable resources at the building

level [4–6]. Due to limited measurements of urban form and district building energy use, the link between the non-physical mechanism of urban morphology and district energy efficiency has still not been explored sufficiently. A better understanding of how or to what extent morphological factors influence building energy consumption and microclimate conditions would provide further insights into energy efficiency practices at the early urban planning stage.

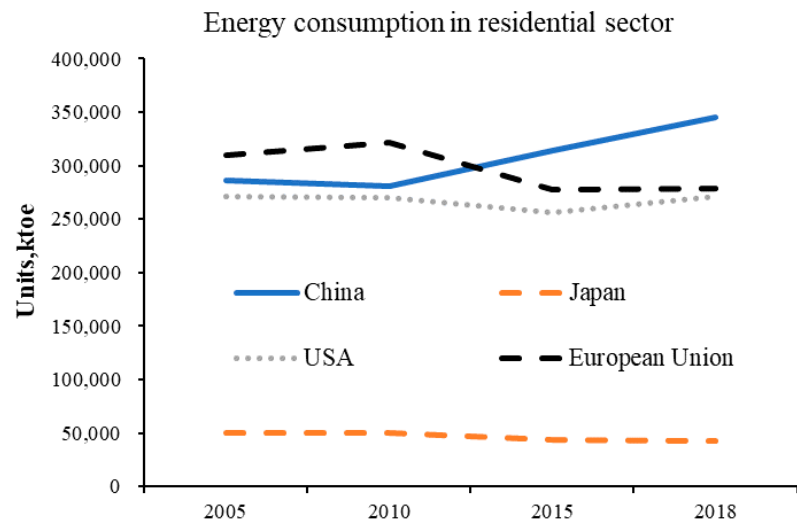


Figure 1. Comparison of energy consumption in residential sectors in China, USA, Japan, and the European Union, datasource: IEA World Energy Balances 2020 [7].

This research is structured as follows: Section 2 presents an overview of related research, and Section 3 introduces the objective and data source. Then, the relationships between urban morphological factors and space heating energy use are investigated, and the validation case is presented in Section 4. Finally, conclusions are drawn.

2. Literature Review

Rapid urbanization and the consequences of a rise in building energy use have raised interest in exploring the link between urban morphology, built local environments and energy efficiency [8–10]. Urban morphology can alter the surrounding environment, and it is commonly known that the urban heat island phenomenon is a consequence of air temperature rises caused by solar energy gain and heat energy emitted into the atmosphere leading to the non-uniform spatial distribution of surface air temperatures. One of the main contributors to this is heat stored by the huge urban thermal mass infrastructures, such as buildings [11,12]. Building thermal load is mainly decided by the net amount of solar energy gain, and conductive and convective energy loss from indoor to the outdoor environment. Urban block typology has been verified to have significant effects on solar heat energy harvesting and operational heating or cooling load intensity [6,13]. Therefore, despite the fact that different building typologies can be implemented under urban planning to achieve the same built urban density, their energy use efficiency may vary significantly [10,14]. This can be explained by the fact that building layout, height, and built density could alter the local thermal environment [15], and building indoor–outdoor heat exchange might modify the amplitude or shift the phase of the surrounding air temperature, in turn, influencing the energy consumption for space heating and cooling. Previous studies indicated that morphological characteristics had a strong modification effect on microclimate, which was highlighted in low-energy urban planning and design [15–17].

Rising building energy use motivates interest in exploring energy-efficient urban design practices. In the early stages of urban or community design, the building energy

modeling tool has been widely used to explore the effects of variables, including a building's physical parameters, orientation, and occupancy patterns on energy demand. An energy simulation tool is generally used in a single building based on typical regional historical weather data, such as the Typical Meteorological Year (TMY), and uses a shading factor to simplify the effect of adjacent buildings on the heat exchange balance. Different urban morphologies could create different situations in their microclimates, in turn, influencing the building's energy consumption performance [18]. Therefore, the building energy simulation model may lead to inaccuracies in a building's energy use simulation without capturing the impact of urban morphology [19,20]. Neglect of the urban microclimate effect may lead to an overestimation of a building's annual heating by 20% and underestimation of cooling load by 30% by EnergyPlus [21]. For instance, Pisello et al. [22] highlighted the inter-building effect on annual energy consumption prediction, with an underestimation of the energy requirement by up to 22% in winter months. Trepci et al. found that inter-building shading effects can lead to a 26% reduction of total building cooling load, highlighting the role of the urban built form in energy conservation [23]. The link between BIM (Building Information Modeling) databases and numerical simulation models could improve the accuracy of urban-scale energy estimations for urban planners at the early design stage [24,25]. One way to capture the impacts of local meteorological conditions on a building's energy consumption is to couple energy load modeling and a modified weather file to increase the accuracy of a building's heating and cooling load simulation [26,27]. Some studies tried to couple the surrounding land model and numerical simulation to improve the accuracy of a building's thermal load modeling [28,29]. Against such a background, the detailed impacts of urban morphology on building energy efficiency and microclimate conditions are essential to reveal, especially for large-scale district central heating supply scenarios.

To date, some studies have investigated the influences of urban morphological attributes on the built environment, and energy efficiency has also been explored based on parametric computer simulation from different perspectives. For example, the research by Shi et al. [30] provided evidence for the interdependencies between street grids and the efficiency of the district cooling system in the high building density city of Singapore, results indicated that block area variable had the largest impacts on capital and operational costs of cooling system. Additionally, correlation analysis in Guangzhou showed that both the sky view factor and pervious surface fraction have significant positive effects on the local-scale urban heat island intensity, whereas only the pervious surface fraction has a positive effect on the local-scale urban wet island intensity [31]. Building typology-induced space heating or cooling energy efficiency is significant [21]. Chen et al. investigated the influence of block building density and height on the heat energy loss rate and found that there is synergistic potential between building density and height, with the effect of building density becoming obvious at relatively low building height conditions [32]. Vartholomaios studied parametric energy on an urban scale, and the results found that a compact perimeter urban block is a more efficient urban form than pavilions and slabs [33]. Simulation results from Kikegawa et al. [34] confirmed that a decreased sky view factor can be an effective measure in reducing building cooling load. According to the simulation results of high-rise building thermal loads, a denser urban context could lower the cooling load by 16–18% [35]. The effect of neighborhoods on COP (coefficient of performance) degradation of the cooling system was verified as significant due to the increase in the local air temperatures [36]. It was suggested that high built density and compact residential building types reduce heat energy demand at the neighborhood scale [15], and similar results in [37] showed that there is a reduction in building heating demand with high built density of up to 40% compared with the low-density neighborhood. The space heating load of a single-family home rises approximately 25% more than a high-rise apartment block constructed with the same insulation level [38]. The study by Leng et al. [24] took 73 office buildings in Harbin as the study objects, using regression analysis to evaluate the influences of different urban morphological factors on heating energy consumption, with

the floor area ratio determined to be the most critical factor in heating energy consumption. The comprehensive effects of urban morphology on the energy consumption and solar radiation access of blocks were evaluated based on Grasshopper simulation, and the optimization approach considering morphological index control and guidance was highlighted in sustainable urban design [39]. Shi et al. concluded that the impact of floor area ratio on exploring solar energy use is dominant [40]. Mangan et al. identified that optimization of building height plays an important role in building energy and economic efficiency [41].

To date, extensive studies have focused on examining the effects of a building's physical parameters, such as construction materials and window–wall ratio, on building energy use. There is still room for further investigation on urban form as an influencing factor on energy efficiency performance [42]. The developments of GIS (geographical information system) and energy use metering provide a solid foundation for the availability of urban morphological factors and district energy use profiles. The data-driven statistical approach enables a quantitative analysis investigating building energy efficiency relating to urban morphological factors, such as building height, built density, and surface-to-volume ratio [17,43]. Due to the general lack of in-depth analysis of the measured energy use, microclimate conditions, and controlled energy supply technologies, such as centralized and decentralized, questions remain regarding the influencing power of urban built form measures on building energy demand [17]. There is a need to help urban planners and energy utilities acquire a better understanding of how and to what extent urban morphology influences energy efficiency.

This study takes Qingdao city as an example and aims at investigating the relationship between urban morphological parameters and measured building heating energy use. The outdoor air temperature variations of selected districts are analyzed before and after the beginning of the central heating supply through on-site measurement. Results are expected to facilitate energy-efficient decision-making in the urban planning field.

3. Material and Methodology

3.1. Study Area

The district central heating supply system is a common heating system in the urban areas of North China. As shown in Figure 2, hot water extracted from a central thermal power plant is delivered through the primary distribution network to a secondary heating station that directly serves individual buildings at a community level. This study was conducted in Qingdao city, located on the east coast of Shandong Peninsula, North China (36° N, 120° E). Its heating season lasts from mid-November to the end of March. Figure 3 presents the daily average outdoor air temperature and solar radiance profiles during the heating period from 2015 to 2016.

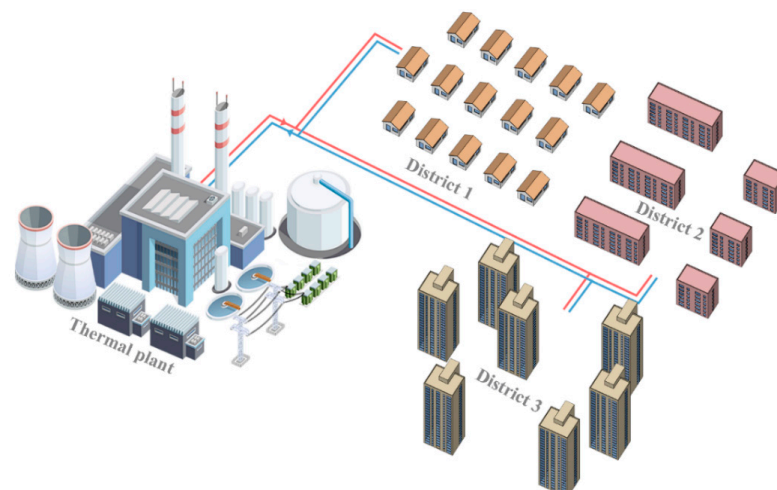


Figure 2. Typical district central heating supply system.

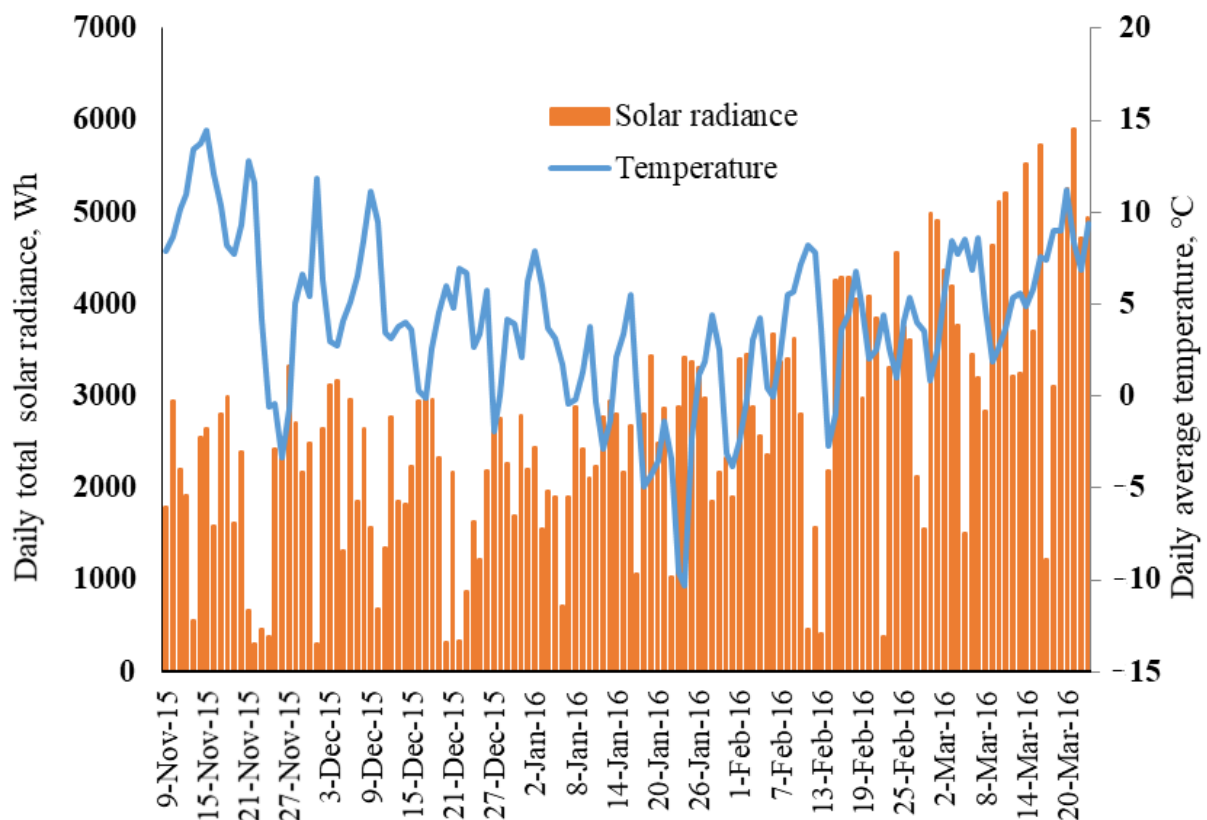


Figure 3. Ambient temperature and daily solar irradiance over the heating season.

3.2. Data Source

Building space heating energy consumption data of more than 200 residential districts were collected, obtained from the district heating company, with most of those building groups built between 2004 and 2008 according to Qingdao residential building energy-efficiency design standards and Qingdao urban planning standards, which can help minimize the effects of other characteristics such as the thermal insulation level. This study focuses on investigating the effect of urban morphology on building heating energy use. In order to minimize the effects of other variables and reveal the role of urban morphology on energy efficiency, residential districts with a total floor area over 40,000 m² were preferred. The spatial distribution of 53 selected residential districts (red block) and the typical building typology in the Qingdao urban area are shown in Figure 4. Detached houses featured with lower building density and high-rise residential apartments present high floor area ratio values. Meanwhile, we obtained the physical parameters of selected residential districts based on the available GIS database, including the block area, average building height, and gross building floor area, as described in Appendix A.

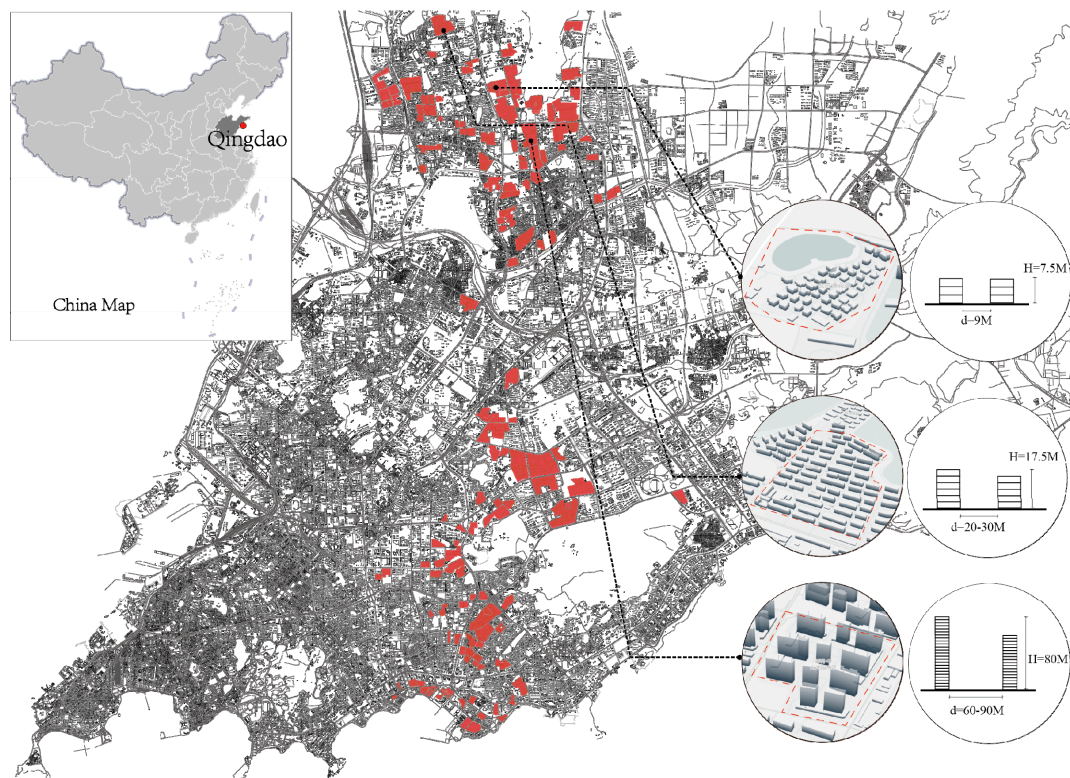


Figure 4. Distribution of selected residential districts, and typical building topology in Qingdao City.

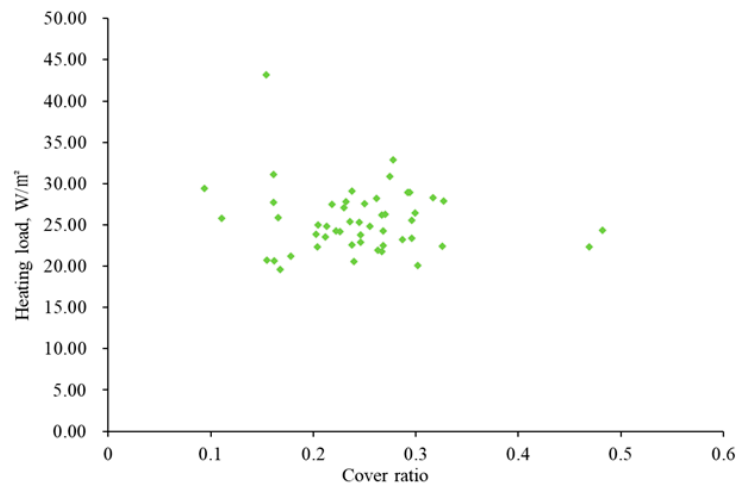
4. Results and Discussion

4.1. Effects of Urban Morphology

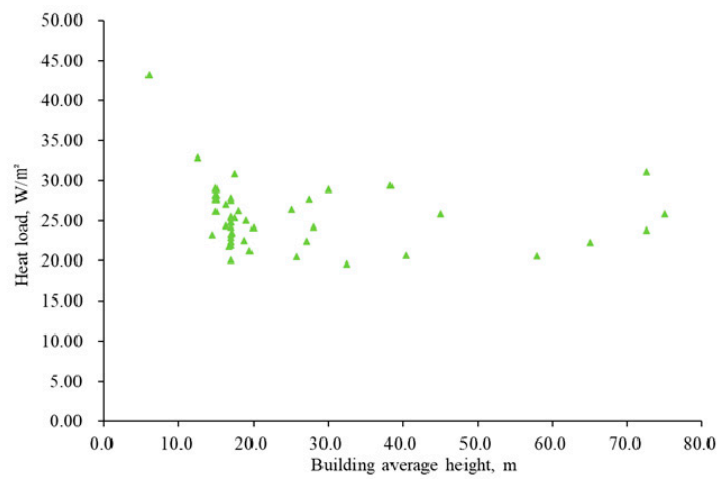
Firstly, we calculated building cover ratio, average building height, and floor area ratio as quantitative characteristics to assess the relationship between urban morphology and district building space heat energy use, as those three variables are common design parameters used in the urban master plan. As shown in Figure 5a, there is a wide range of heat energy use density among the residential districts, and the cover ratio exhibited an insignificant correlation with heat energy use per unit of floor area.

The relationship between building heat energy use and average building height is illustrated in Figure 5b. It does not follow a simple pattern that varies with height range. We observed that the decreasing tendency in heat energy consumption became less (from 20 m to 60 m), and the heat energy use intensity even showed a rising trend when the height is over 60 m, which might be explained by the ratio of building surface exposed to sunlight that reduces the solar radiation absorption. Overall, it presents a negative relationship until a certain threshold, then becomes a positive relationship. Existing studies also indicate that an optimal rise in building height can enhance solar heat reflection and absorption between building surfaces, achieving better exploitation of sun heat [44,45]. Detached houses with a low height featured higher energy loss. A similar pattern could be found in LSE Cities' report [46].

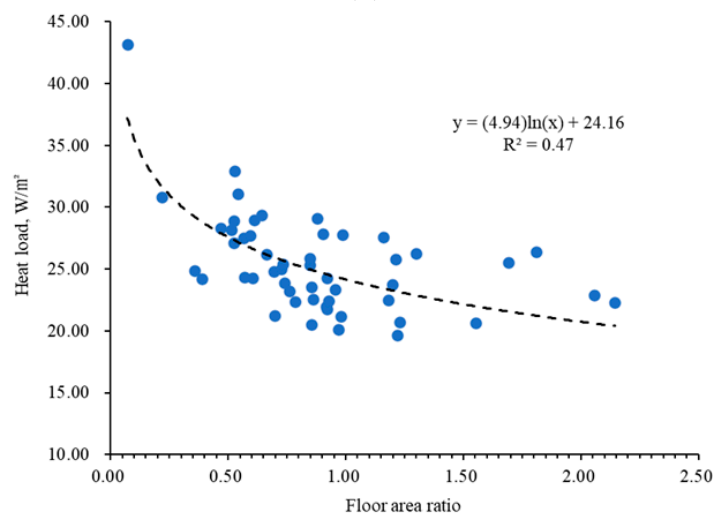
The floor area ratio presents the percentage of the gross building floor area in relation to the size of the block. The variation of the space heating energy use intensity in regards to the floor area ratio is described in Figure 5c. The scatter distribution trend confirms the significant effect of FAR on measured seasonal heating demand. A regression line is presented, and we can observe the clear negative relationship between heat use intensity and FAR value, the induced heat density reduction is notable with rising FAR then the effect becomes less at a large FAR value. For instance, heat energy use density varies from 43.3 W/m^2 to 20.6 W/m^2 when FAR rises from 0.07 to 1.55.



(a)



(b)



(c)

Figure 5. Variations of annual heating demand (heating demand per unit of floor area) with urban morphology factors, building cover ratio (a), building height (b), floor area ratio (c).

4.2. Case Study Validation

4.2.1. Variation of Heating Demand

This part further explores the effects of urban morphology on building heat energy use and the microclimate conditions. This section focuses on analyzing the characteristics of measured district seasonal heating load profiles of selected residential districts as shown in Figure 6. Detailed characteristic parameters of the selected objectives are summarized in Table 1.



Figure 6. Location and exterior view of monitored residential districts, yellow circle points present the positions of temperature sensor.

Table 1. Characteristic parameters of the selected residential districts.

Districts	District Area, 10^4 m ²	Heating Area, 10^4 m ²	FAR	Built Year	Average Height, m
JYSZ	2.1	3.6	1.2	2004	12
HG	8.7	15.7	1.8	2006	60.9
GJCMY	3.9	7.7	2.0	2008	17

Measured daily heat demand profiles of selected districts are shown in Figure 7. The observed variations show the significant dependency on the ambient temperature during the heating seasonal period. As shown in Figure 8, the central heating supply network is adjusted merely based on the supply temperature control approach to avoid fluctuation of hydraulic balance. The measured heating supply temperature shows a linear rising trend with decreasing outdoor air temperature, and the maximum constraints were compensated on the required supply temperature when the ambient temperature decreased further. The amount of heat transported could be calculated by water mass and the temperature difference between water supply and return. The distribution of the temperature difference reveals the variations of operational heating demand over the whole heating period. To ensure that the results are comparable, we normalized the measured

temperature differences between supply and return water over the heating season as shown in Figure 9. Generally, 9 November to 15 November is the heating trial operation period, and the sub-station serves the district space heating with ultra-low water temperature, approximately 35 °C.

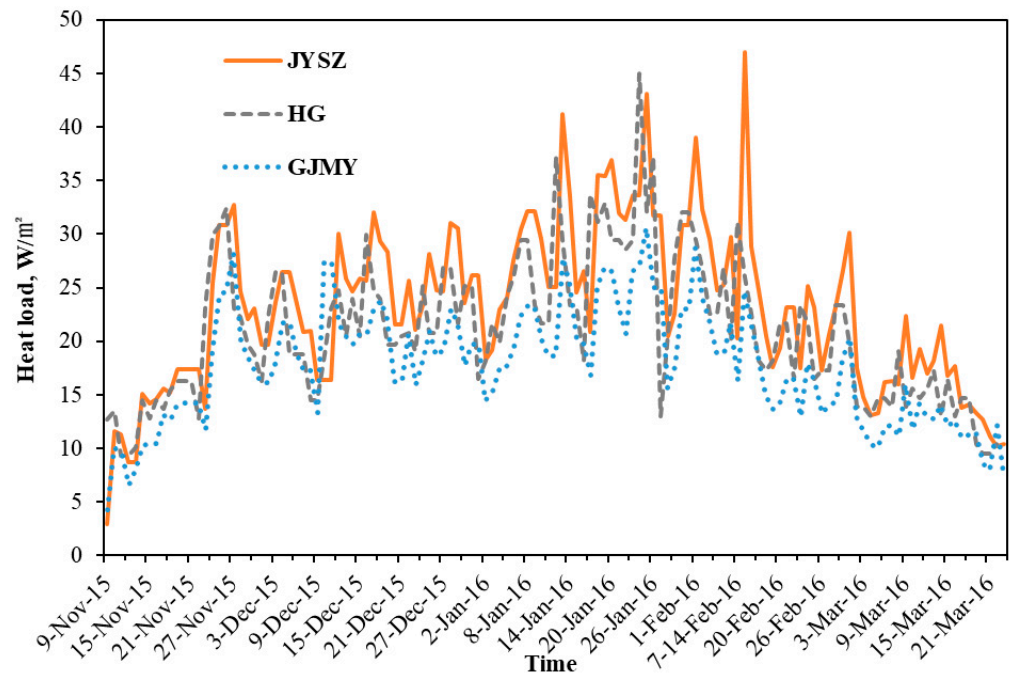


Figure 7. Measured district heat load profiles over the heating period.

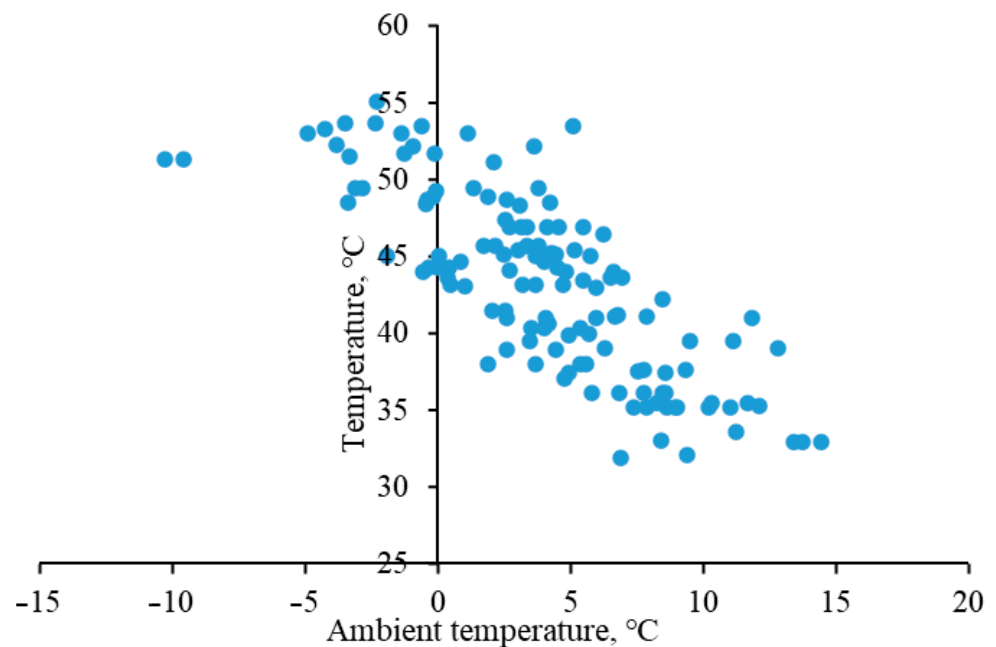


Figure 8. Hot water supply temperature as a function of ambient temperature.

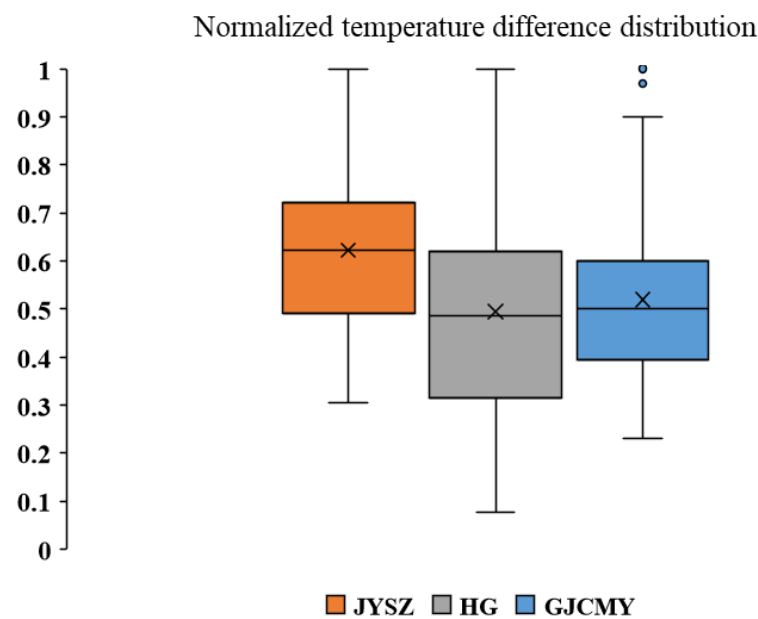


Figure 9. Distributions of normalized temperature difference between supply and return hot water.

As illustrated in Figure 10a–c, scatter shows the color-scale distributions of historical heat energy use density over 129 days in JYSZ (Figure 10a), HG (Figure 10b), and GJCMY (Figure 10c). There are considerable variations in daily district heating loads, and it can be confirmed that heating demand is a function of daily average ambient temperature and total solar radiance. Overall, space heating demand presents a decreasing trend with increasing ambient temperature and solar radiance values.

We used the multi-factor line regression approach to examine the effects of ambient temperature and solar radiance on district space heating demand. In order to deal with the values that lie in different ranges, we normalized variables to 0 to 1 range respectively. The regression model can be expressed as:

$$y = b_0 + b_1 \times x_1 + b_2 \times x_2 \quad (1)$$

where, x_1 presents daily average ambient temperature, x_2 is daily total solar radiance.

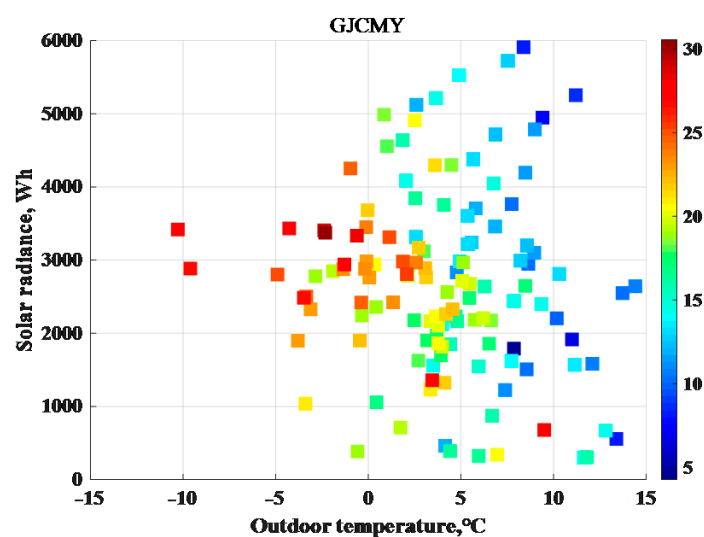


Figure 10. Cont.

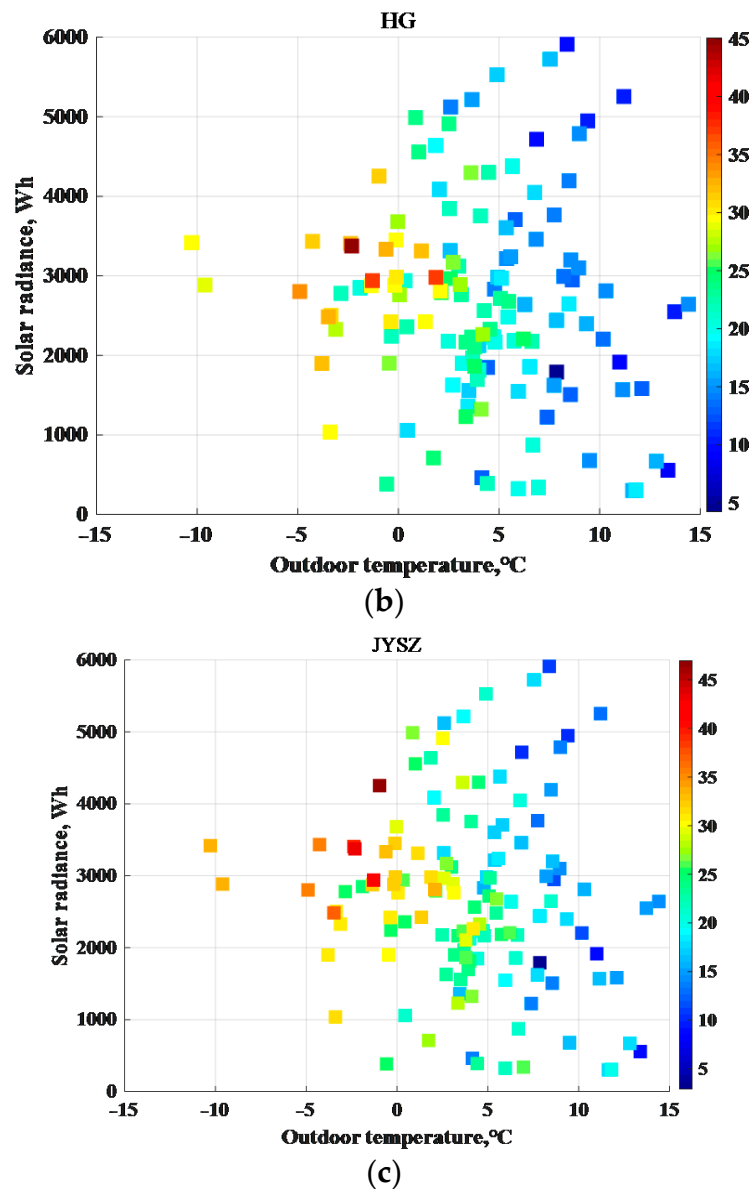


Figure 10. Color-scale distributions of heating energy demand (W/m^2) of selected districts under different weather conditions: JYSZ (a), HG (b), GJCMY (c).

Table 2 shows the regression results, with outdoor air temperature presenting the most significant impact on the building space heating energy consumption. The heating load of GJCMY was more sensitive to the solar radiance, and a high FAR value enabled the building to gain more solar heat energy in reducing building heating demand.

Table 2. Results of the regression analysis for heating load.

Variables	JYSZ	HG	GJCMY
b0	0.63	0.60	0.77
b1	−0.41	−0.38	−0.44
b2	−0.01	−0.07	−0.15
R-square statistic	0.62	0.59	0.58

4.2.2. Scenarios of Outdoor Air Temperature Profile

Surface temperatures at heights of 2.0 m above the ground in selected districts were measured with a Thermo Recorder TR-72wf with measurement accuracy ± 0.5 °C and a 0.1 °C resolution. The measurement scenario is shown in Figure 6. In order to avoid disturbance from direct solar radiation, positions were placed 2.0 m near the building. Outdoor temperature measurements data with 10-min intervals were taken during three different periods before and after the operational stage of central heating supply in November, 2020. The three periods were categorized as follows: non-heating period, heating trial operation stage (low-temperature hot water supply) and heating period. This enabled the exploration and comparison of the effects of different heat emitters on local ambient temperature profiles.

The outdoor temperature variations with time on 2 November 2020 (non-heating day) were illustrated in Figure 11, the measured temperature of mid-rise residential areas was generally higher than the high-rise residential district. Open high-rise residential district HG featured with a larger temperature drop rate during the night period. The measured temperature difference between the high-rise and mid-rise districts were more obvious at night, it was about 1.2 °C at 3:30 a.m. in 2 November. The maximum measured temperature of the HG district during the daytime was about 1 °C lower than the two mid-rise districts.

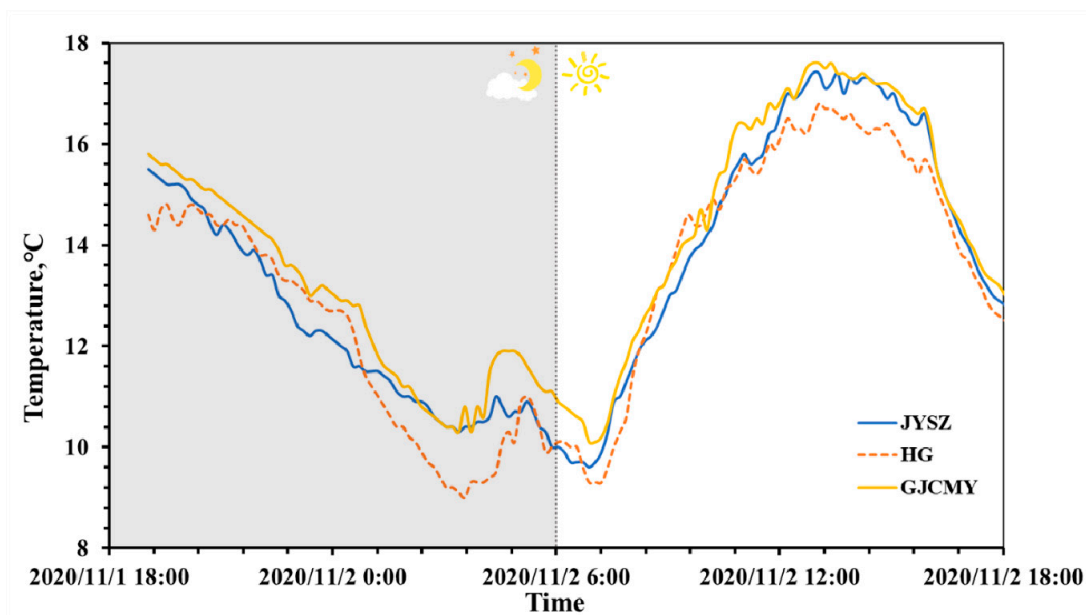


Figure 11. Variations of outdoor temperature profiles during non-heating time.

Comparisons of measured time series temperature profiles on heating trial days with low heating temperature operation are shown in Figure 12. The temperature differences between high-rise and mid-rise districts became less in comparison with non-heating supply time. The high-rise district still presented the lowest daily measured outdoor temperature, its temperature drop rate was decreased at night due to energy release from the surrounding buildings.

The profiles of outdoor temperature during heating days are shown in Figure 13. In comparison with the scenarios described in Figures 11 and 12, the increasing heat energy supply density altered the microclimates of selected residential districts further. It is clear that the surrounding temperature of high-rise district HG had increased obviously, outdoor temperature points of HG were almost consistent with mid-rise JYSZ district on an average level, and their maximum daily temperature was almost the same. Meanwhile, the measured temperature points of compact GJCMY with larger FAR were obviously higher than HG and JYSZ districts at night times without the effects of solar radiation. From

the identified temperature difference, it can be concluded that the operation of district space heating reshaped the local air temperature. FAR became an important contributor in reshaping the outdoor temperature, especially during the night period.

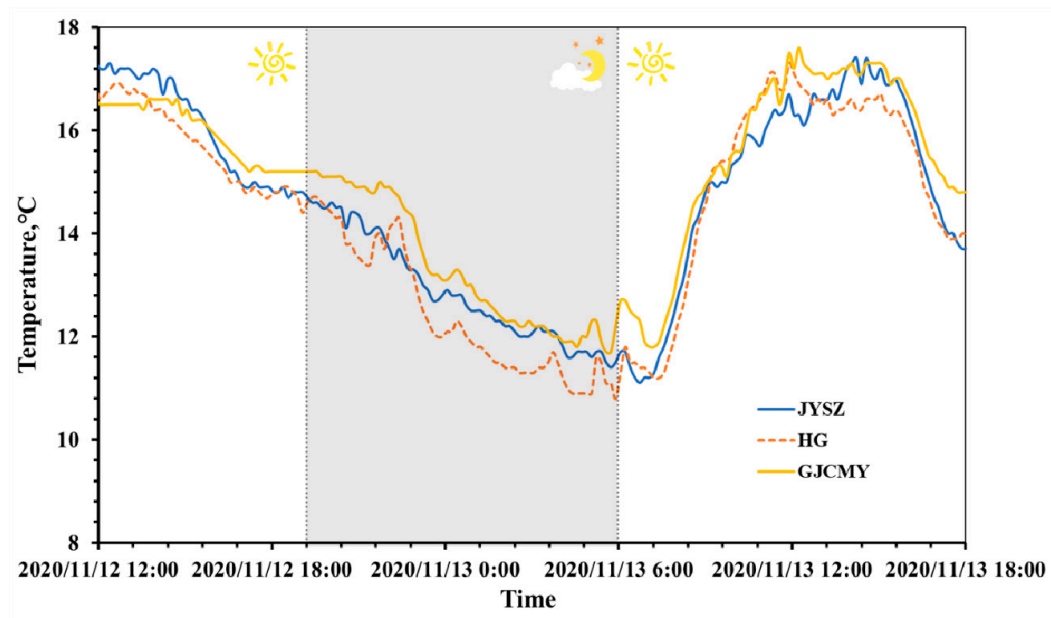


Figure 12. Variations of outdoor temperature profiles during heating trial operational stage.

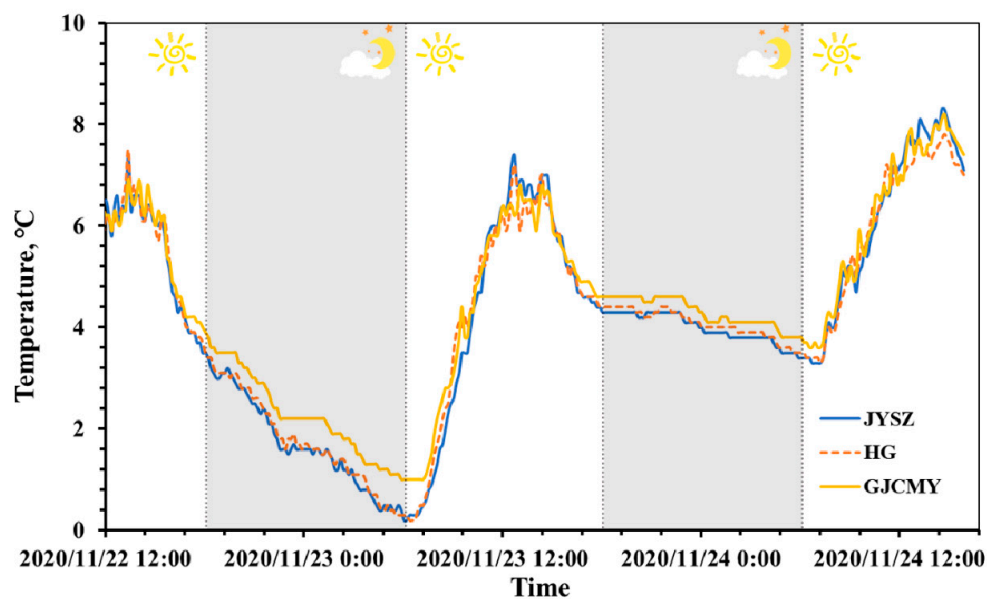


Figure 13. Variations of outdoor temperature profiles during central heating time.

We presented the daily maximum temperature, minimum temperature, and their differences to compare the effects of urban morphology on local climate conditions as shown in Figure 14. High-rise district (HG) showed the lowest minimum temperature under non or low-temperature heating supply days, and its level could be raised to the same level with JYSZ under heating supply days. On a cold day (23 November), the damping effect on the measured district temperature difference is more obvious with rising FAR.

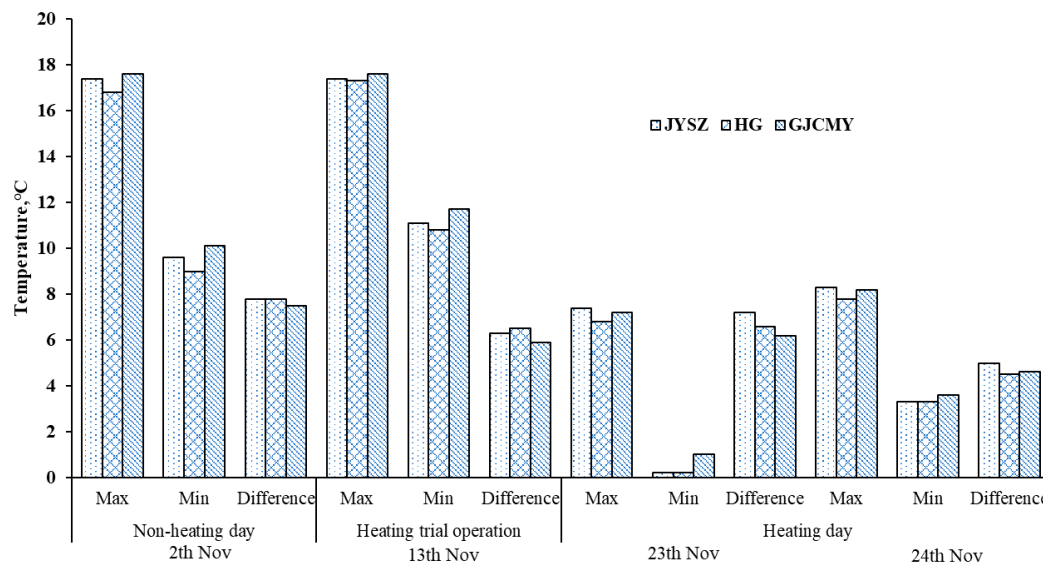


Figure 14. Comparisons of measured maximum and minimum outdoor temperature, daily temperature differences among selected districts.

5. Conclusions

The building sector accounts for a significant proportion of social energy consumption. This study presents a quantitative and comparative analysis to reveal the effects of morphological factors on the residential district space heating performance in Qingdao City, and outdoor meteorological situations were also compared through on-site measurement. Some conclusions can be drawn as follows:

First, this study provides an investigation of the relationship between urban form parameters with building space heating energy performance based on the measured heat energy consumption of selected residential districts. Results indicate that an initial rise in building height could decrease the heat energy use significantly. FAR shows the greatest impact on heat energy use density, and it is worth noticing that districts with a larger FAR value achieve higher space heating efficiency.

Results of the validation case further investigated the characteristics of the heat demand profiles of selected residential districts, and regression analysis indicates that the heat energy use density of residential districts with a higher built density is influenced more by solar radiation.

A comparison of the external thermal environment of selected districts was carried out through on-site measurement before and after the operational stage of district central heating supply. Changes in minimum, maximum and average outdoor air temperature profiles of residential districts were identified. Accordingly, the heat energy loss of the buildings during the heating period can increase the surrounding ambient temperature, and the increase in outdoor temperature is more obvious in a residential district with a high FAR value during the night period.

The findings help bridge the knowledge gap between urban morphology and heat-energy efficiency, and they are expected to help facilitate decision-making at the initial stage of urban planning. With more multidisciplinary collaboration, further measurement of more recent building energy use and microclimate conditions are recommended to enhance the understanding of the extent to which the central heating supply alters the district microclimate under different urban morphologies.

Author Contributions: Methodology, Y.L.; software, D.W.; validation, D.W. and S.L.; formal analysis, Y.L.; investigation, D.W. and S.L.; resources, Y.L.; data curation, Y.L. and D.W.; writing—original

draft preparation, Y.L.; writing—review and editing, Y.L.; visualization, W.G. All authors have read and agreed to the published version of the manuscript.

Funding: This research was funded by “China National Key R&D Program Research on the energy efficiency and health performance improvement of building operations based on lifecycle carbon emissions reduction, grant number 2018YFE0106100” and “Shandong Province Key R&D Program on Development of the Healthy and Low-carbon Residential House with Smart Home Environment Management System, grant number 2019GSF110003”.

Institutional Review Board Statement: Not applicable.

Informed Consent Statement: Not applicable.

Data Availability Statement: Not applicable.

Conflicts of Interest: The authors declare no conflict of interest.

Appendix A

Table A1. Information on selected residential districts.

No. of District	District Area, m ²	Building Area, m ²	Cover Ratio	Average Height, m	FAR	Heating Load, W/m ²
D1	64,293	76,971	0.25	19.50	1.20	23.76
D2	224,976	127,477	0.22	17.00	0.57	27.52
D3	209,035	74,551	0.21	17.00	0.36	24.85
D4	175,462	52,867	0.20	12.50	0.30	24.96
D5	172,724	146,294	0.25	17.50	0.85	25.33
D6	171,510	80,021	0.32	15.00	0.47	28.31
D7	167,319	153,855	0.27	16.70	0.92	21.79
D8	142,519	121,911	0.21	17.10	0.86	23.53
D9	138,615	53,714	0.23	20.00	0.39	24.19
D10	129,935	123,963	0.30	17.00	0.95	23.38
D11	129,446	67,751	0.23	16.30	0.52	27.10
D12	128,204	100,702	0.20	17.00	0.79	22.36
D13	120,764	111,097	0.27	17.00	0.92	24.25
D14	120,242	62,953	0.29	15.00	0.52	28.91
D15	111,170	94,048	0.17	45.00	0.85	25.86
D16	107,379	124,526	0.25	15.00	1.16	27.60
D17	107,281	56,538	0.28	12.50	0.53	32.92
D18	106,998	74,771	0.18	19.50	0.70	21.24
D19	103,530	127,287	0.16	40.40	1.23	20.71
D20	100,344	51,517	0.26	15.00	0.51	28.18
D21	93,417	92,126	0.23	15.00	0.99	27.80
D22	87,320	58,426	0.29	15.00	0.67	20.53
D23	83,078	45,070	0.16	72.50	0.54	31.10
D24	82,843	140,084	0.30	17.00	1.69	25.52
D25	79,627	123,577	0.16	57.80	1.55	20.62
D26	79,450	96,406	0.11	75.00	1.21	25.82
D27	77,992	54,152	0.26	17.00	0.69	24.84
D28	74,068	53,724	0.21	19.00	0.73	25.02
D29	73,636	5245	0.15	6.00	0.07	43.16
D30	72,133	41,016	0.48	16.30	0.57	24.38
D31	70,805	64,816	0.26	17.00	0.92	21.97
D32	65,429	47,985	0.24	17.00	0.73	25.38
D33	61,665	65,057	0.23	72.50	1.06	13.61
D34	57,977	34,465	0.16	27.50	0.59	27.72
D35	57,922	49,434	0.24	25.70	0.85	20.53
D36	55,775	48,907	0.24	15.00	0.88	29.09
D37	54,307	49,050	0.33	17.00	0.90	27.88

Table A1. Cont.

No. of District	District Area, m ²	Building Area, m ²	Cover Ratio	Average Height, m	FAR	Heating Load, W/m ²
D38	50,667	37,374	0.28	17.50	0.74	23.86
D39	49,196	31,652	0.20	72.50	0.64	29.39
D40	48,795	37,037	0.09	38.30	0.76	23.22
D41	48,683	88,004	0.29	14.50	1.81	26.43
D42	48,503	57,192	0.30	25.00	1.18	22.49
D43	46,267	27,957	0.27	17.00	0.60	24.25
D44	46,264	39,835	0.22	28.10	0.86	22.57
D45	45,162	41,795	0.24	18.80	0.93	22.45
D46	43,932	57,055	0.33	27.10	1.30	26.28
D47	43,347	41,969	0.27	18.00	0.97	20.12
D48	43,207	88,777	0.30	17.00	2.05	22.92
D49	42,718	91,603	0.25	17.00	2.14	22.33
D50	42,716	52,005	0.47	65.00	1.22	19.64
D51	42,411	28,062	0.17	32.50	0.66	26.18
D52	40,526	24,677	0.27	15.00	0.61	28.95
D53	40,099	39,285	0.29	30.00	0.98	21.17

References

- Hong, T.; Chen, Y.; Luo, X.; Luo, N.; Lee, S.H. Ten questions on urban building energy modeling. *Build. Environ.* **2020**, *168*, 106508. [CrossRef]
- Nations, U. Sustainable Development Goals, Goal 11: Make Cities Inclusive, Safe, Resilient and Sustainable. Available online: <https://www.un.org/sustainabledevelopment/cities/> (accessed on 10 January 2021).
- Building energy conservation research center, *Annual Report on China Building Energy Efficiency, 2020*; China Architecture & Building Press: Beijing, China, 2020.
- Streicher, K.N.; Padey, P.; Parra, D.; Bürer, M.C.; Schneider, S.; Patel, M.K. Analysis of space heating demand in the Swiss residential building stock: Element-based bottom-up model of archetype buildings. *Energy Build.* **2019**, *184*, 300–322. [CrossRef]
- Yang, X.; Svendsen, S. Ultra-low temperature district heating system with central heat pump and local boosters for low-heat-density area: Analyses on a real case in Denmark. *Energy* **2018**, *159*, 243–251. [CrossRef]
- Zhang, J.; Xu, L.; Shabunko, V.; Tay, S.E.R.; Sun, H.; Lau, S.S.Y.; Reindl, T. Impact of urban block typology on building solar potential and energy use efficiency in tropical high-density city. *Appl. Energy* **2019**, *240*, 513–533. [CrossRef]
- IEA. IEA World Energy Balances 2020. World Energy Balances and Statistics. Available online: <https://www.iea.org/subscribe-to-data-services/world-energy-balances-and-statistics> (accessed on 8 February 2021).
- Zhang, J.; Cui, P.; Song, H. Impact of urban morphology on outdoor air temperature and microclimate optimization strategy base on Pareto optimality in Northeast China. *Build. Environ.* **2020**, *180*, 107035. [CrossRef]
- Yang, Z.; Chen, Y.; Zheng, Z.; Huang, Q.; Wu, Z. Application of building geometry indexes to assess the correlation between buildings and air temperature. *Build. Environ.* **2020**, *167*, 106477. [CrossRef]
- Chen, H.-C.; Han, Q.; de Vries, B. Urban morphology indicator analyzes for urban energy modeling. *Sustain. Cities Soc.* **2020**, *52*, 101863. [CrossRef]
- Duan, S.; Luo, Z.; Yang, X.; Li, Y. The impact of building operations on urban heat/cool islands under urban densification: A comparison between naturally-ventilated and air-conditioned buildings. *Appl. Energy* **2019**, *235*, 129–138. [CrossRef]
- He, B.-J.; Wang, J.; Liu, H.; Ulpiani, G. Localized synergies between heat waves and urban heat islands: Implications on human thermal comfort and urban heat management. *Environ. Res.* **2021**, *193*, 110584. [CrossRef] [PubMed]
- Cody, B.; Loeschig, W.; Eberl, A. Operating energy demand of various residential building typologies in different European climates. *Smart Sustain. Built Environ.* **2018**, *7*, 226–250. [CrossRef]
- Shi, L.; Luo, Z.; Matthews, W.; Wang, Z.; Li, Y.; Liu, J. Impacts of urban microclimate on summertime sensible and latent energy demand for cooling in residential buildings of Hong Kong. *Energy* **2019**, *189*, 116208. [CrossRef]
- Rode, P.; Keim, C.; Robazza, G.; Viejo, P.; Schofield, J. Cities and Energy: Urban Morphology and Residential Heat-Energy Demand. *Environ. Plan. B: Plan. Des.* **2014**, *41*, 138–162. [CrossRef]
- He, B.-J.; Ding, L.; Prasad, D. Relationships among local-scale urban morphology, urban ventilation, urban heat island and outdoor thermal comfort under sea breeze influence. *Sustain. Cities Soc.* **2020**, *60*, 102289. [CrossRef]
- Steadman, P.; Hamilton, I.; Evans, S. Energy and urban built form: An empirical and statistical approach. *Build. Res. Inf.* **2014**, *42*, 17–31. [CrossRef]
- Taleghani, M.; Kleerekoper, L.; Tenpierik, M.; van den Dobbela, A. Outdoor thermal comfort within five different urban forms in the Netherlands. *Build. Environ.* **2015**, *83*, 65–78. [CrossRef]

19. Javanroodi, M.N. Impacts of Microclimate Conditions on the Energy Performance of Buildings in Urban Areas. *Buildings* **2019**, *9*, 189. [[CrossRef](#)]
20. Vuckovic, M.; Kiesel, K.; Mahdavi, A. The Extent and Implications of the Microclimatic Conditions in the Urban Environment: A Vienna Case Study. *Sustainability* **2017**, *9*, 177. [[CrossRef](#)]
21. Boccalatte, A.; Fossa, M.; Gaillard, L.; Menezo, C. Microclimate and urban morphology effects on building energy demand in different European cities. *Energy Build.* **2020**, *224*, 110129. [[CrossRef](#)]
22. Pisello, A.L.; Taylor, J.E.; Xu, X.; Cotana, F. Inter-building effect: Simulating the impact of a network of buildings on the accuracy of building energy performance predictions. *Build. Environ.* **2012**, *58*, 37–45. [[CrossRef](#)]
23. Trepci, E.; Maghelal, P.; Azar, E. Urban built context as a passive cooling strategy for buildings in hot climate. *Energy Build.* **2021**, *231*, 110606. [[CrossRef](#)]
24. Leng, H.; Chen, X.; Ma, Y.; Wong, N.H.; Ming, T. Urban morphology and building heating energy consumption: Evidence from Harbin, a severe cold region city. *Energy Build.* **2020**, *224*, 110143. [[CrossRef](#)]
25. Pasichnyi, O.; Wallin, J.; Kordas, O. Data-driven building archetypes for urban building energy modelling. *Energy* **2019**, *181*, 360–377. [[CrossRef](#)]
26. Allegrini, J.; Orehounig, K.; Mavromatidis, G.; Ruesch, F.; Dorer, V.; Evins, R. A review of modelling approaches and tools for the simulation of district-scale energy systems. *Renew. Sustain. Energy Rev.* **2015**, *52*, 1391–1404. [[CrossRef](#)]
27. He, J.; Hoyano, A.; Asawa, T. A numerical simulation tool for predicting the impact of outdoor thermal environment on building energy performance. *Appl. Energy* **2009**, *86*, 1596–1605. [[CrossRef](#)]
28. Wang, Y.-C.; Bian, Z.-F.; Qin, K.; Zhang, Y.; Lei, S.-G. A modified building energy model coupled with urban parameterization for estimating anthropogenic heat in urban areas. *Energy Build.* **2019**, *202*, 109377. [[CrossRef](#)]
29. Samuelson, H.; Claussnitzer, S.; Goyal, A.; Chen, Y.; Romo-Castillo, A. Parametric energy simulation in early design: High-rise residential buildings in urban contexts. *Build. Environ.* **2016**, *101*, 19–31. [[CrossRef](#)]
30. Shi, Z.; Hsieh, S.; Fonseca, J.A.; Schlueter, A. Street grids for efficient district cooling systems in high-density cities. *Sustain. Cities Soc.* **2020**, *60*, 102224. [[CrossRef](#)]
31. Jin, L.; Pan, X.; Liu, L.; Liu, L.; Liu, J.; Gao, Y. Block-based local climate zone approach to urban climate maps using the UDC model. *Build. Environ.* **2020**, *186*, 107334. [[CrossRef](#)]
32. Chen, Y.; Wu, J.; Yu, K.; Wang, D. Evaluating the impact of the building density and height on the block surface temperature. *Build. Environ.* **2020**, *168*, 106493. [[CrossRef](#)]
33. Vartholomaios, A. A parametric sensitivity analysis of the influence of urban form on domestic energy consumption for heating and cooling in a Mediterranean city. *Sustain. Cities Soc.* **2017**, *28*, 135–145. [[CrossRef](#)]
34. Kikegawa, Y.; Genchi, Y.; Kondo, H.; Hanaki, K. Impacts of city-block-scale countermeasures against urban heat-island phenomena upon a building's energy-consumption for air-conditioning. *Appl. Energy* **2006**, *83*, 649–668. [[CrossRef](#)]
35. Lima, I.; Scalco, V.; Lamberts, R. Estimating the impact of urban densification on high-rise office building cooling loads in a hot and humid climate. *Energy Build.* **2019**, *182*, 30–44. [[CrossRef](#)]
36. Gracik, S.; Heidarinejad, M.; Liu, J.; Srebric, J. Effect of urban neighborhoods on the performance of building cooling systems. *Build. Environ.* **2015**, *90*, 15–29. [[CrossRef](#)]
37. Trigaux, D.; Oosterbosch, B.; De Troyer, F.; Allacker, K. A design tool to assess the heating energy demand and the associated financial and environmental impact in neighbourhoods. *Energy Build.* **2017**, *152*, 516–523. [[CrossRef](#)]
38. Tereci, A.; Ozkan, S.T.E.; Eicker, U. Energy benchmarking for residential buildings. *Energy Build.* **2013**, *60*, 92–99. [[CrossRef](#)]
39. Xia, B.; Li, Z. Optimized methods for morphological design of mesoscale cities based on performance analysis: Taking the residential urban blocks as examples. *Sustain. Cities Soc.* **2021**, *64*, 102489. [[CrossRef](#)]
40. Shi, Z.; Fonseca, J.A.; Schlueter, A. A parametric method using vernacular urban block typologies for investigating interactions between solar energy use and urban design. *Renew. Energy* **2021**, *165*, 823–841. [[CrossRef](#)]
41. Mangan, S.D.; Koclar Oral, G.; Erdemir Kocagil, I.; Sozen, I. The impact of urban form on building energy and cost efficiency in temperate-humid zones. *J. Build. Eng.* **2021**, *33*, 101626. [[CrossRef](#)]
42. Ahn, Y.; Sohn, D.-W. The effect of neighbourhood-level urban form on residential building energy use: A GIS-based model using building energy benchmarking data in Seattle. *Energy Build.* **2019**, *196*, 124–133. [[CrossRef](#)]
43. Chen, H.-C.; Han, Q.; De Vries, B. Modeling the spatial relation between urban morphology, land surface temperature and urban energy demand. *Sustain. Cities Soc.* **2020**, *60*, 102246. [[CrossRef](#)]
44. Song, S.; Leng, H.; Xu, H.; Guo, R.; Zhao, Y. Impact of Urban Morphology and Climate on Heating Energy Consumption of Buildings in Severe Cold Regions. *Int. J. Environ. Res. Public Health* **2020**, *17*, 8354. [[CrossRef](#)] [[PubMed](#)]
45. Zhu, D.; Song, D.; Shi, J.; Fang, J.; Zhou, Y. The Effect of Morphology on Solar Potential of High-Density Residential Area: A Case Study of Shanghai. *Energies* **2020**, *13*, 2215. [[CrossRef](#)]
46. Cities, L. *Cities and Energy: Urban Morphology and Heat Energy Demand Final Report*; LSE Cities: London, UK, 2014.